Dissipation and tunneling in heavy-ion reactions near the Coulomb barrier

E. Piasecki,[1,*] M. Kowalczyk,[1] S. Yusa,[2] A. Trzcińska,[1] and K. Hagino[2,3]
[1]*Heavy Ion Laboratory, University of Warsaw, Poland*
[2]*Department of Physics, Tohoku University, Sendai 980-8578, Japan*
[3]*Research Center for Electron Photon Science, Tohoku University, 1-2-1 Mikamine, Sendai 982-0826, Japan*

(Received 16 February 2019; published 26 July 2019)

Influence of couplings to collective excitations on fusion process has been well established experimentally and theoretically. Much less is known about the influence of dissipation caused by transfer reactions, even less due to noncollective excitations. In this paper, we report the results of the comparison of experimental barrier distributions with the CC + RMT model calculations taking into account noncollective excitations, in which the stationary coupled channels method is merged with a statistical approach based on the random matrix theory. In spite of many assumptions and approximations, we find that the model works well for medium systems without fitting parameters, describing the influence of dissipation on tunneling. On the other hand, for heavier systems this mechanism does not appear to be sufficient. This points to the importance of other dissipation mechanisms for these systems, such as nucleon transfer processes.

DOI: 10.1103/PhysRevC.100.014616

I. INTRODUCTION

The basic mechanism of heavy-ion fusion reactions can be described in terms of a central potential, which depends on the distance between the centers-of-mass of the target and projectile nuclei. At some distance the potential has its maximum value, which is referred to as the Coulomb barrier height. It arises from the competition between the long-range repulsive Coulomb force and the short-ranged attractive nuclear force. A fusion event requires that the two interacting nuclei overcome or penetrate through this barrier.

It has been known that the relative motion between the projectile and target nuclei couples to internal degrees of freedom of the two interacting nuclei, frequently leading to generation of a barrier distribution [1–3]. In other words, a single value of the barrier height gets replaced by a barrier distribution (BD), $D_{\rm fus}$, resulting in a strong enhancement of fusion cross sections at sub-barrier energies in comparison with the result of a simple potential penetration model. In some cases, one observes a prominent structure in a distribution, providing a fingerprint of the couplings involved during fusion reactions [1,4].

The barrier distribution, $D_{\rm fus}$, can be determined both experimentally and theoretically studying the energy derivative of barrier penetrability and may be obtained directly from fusion excitation function measurements through the relation [5]:

$$D_{\rm fus} \equiv \frac{d^2}{dE^2}(E\sigma_{\rm fus}), \tag{1}$$

where $\sigma_{\rm fus}$ is the fusion cross section and E is the incident energy in the center-of-mass (c.m.) frame.

However, fusion measurements are often rather difficult and require expensive instrumentation. Since the barrier transmission and reflection are complementary to each other, there exists an alternative method to measure the barrier height distribution, namely registering the ions, which do not penetrate the barrier, but are quasielastically reflected from the barrier [6]. More specifically, one has to register at backward angles the sum of elastic and inelastic scattering, transfers, and break-up events, without necessity of identifying particular reaction channels. It has been shown [6] that the cross section for quasielastic scattering, $\sigma_{\rm qe}$, measured at backward angles, normalized to the cross section for Rutherford scattering, $\sigma_{\rm Ruth}$, gives the barrier distribution via the following formula [6–8]:

$$D_{\rm qe}(E) \equiv -\frac{d}{dE}\left[\frac{\sigma_{\rm qe}}{\sigma_{\rm Ruth}}(E)\right]. \tag{2}$$

Theoretically, the barrier distribution can be calculated in the framework of the coupled-channels (CC) method. The CC calculations usually well account for experimental results, in particular, enhancement of fusion cross sections below the barrier. Still, the method has some open problems. The model parameters should be fitted to experimental results or taken from systematics, as they are difficult to calculate microscopically. Although this concerns in particular parameters of the imaginary part of the potential, even the real part, usually postulated to have a Woods-Saxon (W-S) form, differs in the value of diffuseness parameter a for describing the fusion or scattering data [9–11]. This results in that the predictive power of the CC method is rather limited. Moreover, the role of imaginary potential is to describe all effects connected with the inelasticity of interaction taken together: fusion, inelastic excitations (including DIC), transfers, breakups. This would

*piasecki@fuw.edu.pl

make it difficult to theoretically identify different reaction channel contributions.

Another problem has been noticed when we tried to use the CC method to describe the barrier distribution obtained in the series of our experiments with ^{20}Ne interacting with ^{58,60,61}Ni, ^{90,92}Zr, ^{118,119,122}Sn, and ^{208}Pb [12–17]. Namely, the conventional CC calculations, including collective excitations of Ne and all employed targets, predict that, due to the very strong ^{20}Ne deformation, the barrier distribution is determined essentially by properties of this projectile. In particular, for every medium and heavy target the BD is predicted to possess a structure, i.e., more than one peak. Experimentally, however, the structure was observed only for the ^{58,60}Ni and ^{90}Zr targets, while for the other target nuclei it was smoothed out. It was in contrary to the expectations that if one uses the same projectile, which dominates the shape of barrier distribution, as in the case ^{20}Ne $+^{90,92}$Zr, one would obtain very similar barrier distribution, $D_{\rm qe}$. However, the experiment showed a significant target dependence, which pointed to some deficiency of the model.

Can smoothing of the BD structure be caused by coupling to transfer channels? In general, this is still an open question (for a discussion of various approaches see Ref. [18] and references therein). However, when using the ^{20}Ne beam, we observed a striking difference between $D_{\rm qe}$ for the ^{90}Zr and that for the ^{92}Zr targets, in spite of the fact the total light particle transfer cross sections at backward angle for near barrier energies turned out to be small and very similar [14].

The above argument against attributing to the transfer channels the smoothing out the BD structure in the ^{20}Ne + ^{92}Zr system have been strongly supported by our measurements of BD in the ^{20}Ne + ^{58,60,61}Ni systems. Namely, while for the ^{58,60}Ni targets the structure is visible, in the case of ^{61}Ni it is smoothed out [12]. Concerning the experimental transfer cross sections, they are not only much smaller than in the ^{20}Ne + ^{90}Zr case (where the structure is visible), but also similar among the three Ni isotopes, with exception of the little bit larger $1n$ pick-up cross section for the ^{61}Ni target. According to many authors, e.g., [18–20], the transfer influences fusion mainly via $1n$ and $2n$ channels, so should be significant mainly when the ground-state-to-the-ground-state Q value, Q_{gg}, for these channels, are positive. However, the Q_{gg} in case of the all these Ni isotopes are negative. Moreover, the $1n$ transfer channel in the ^{20}Ne + ^{61}Ni case is a pretty rare case in which calculation of transfer impact within the CC method in the fully quantal way was feasible and it turned out [13] that it practically did not influence the shape of the $D_{\rm qe}$ distribution. This points to the other reasons of difference in shapes of barrier distributions, evidently connected with target nuclei, and a natural guess is the influence of other weak channels, namely of noncollective excitations.

This is the hypothesis we advanced in the paper [14]: the differences in barrier distributions can originate from the influence of weak but numerous couplings to noncollective excitations, which are different in various targets. For example, due to the fact that the ^{92}Zr target has two neutrons outside the $N = 50$ closed shell in ^{90}Zr, for the same excitation energy the level density of the former nucleus is about an order of magnitude higher than that of the latter one. This should result in the much stronger effect of coupling to noncollective excitations in the ^{92}Zr nucleus. Also in the case of Ni isotopes, the level density of ^{61}Ni is much higher than of the ^{58,60}Ni isotopes (see Fig. 1 in Ref. [12]).

Usually in CC calculations only strong reaction channels, i.e., collective excitations, are taken into account. Weak reaction channels, such as transfer and single-particle excitations, except for the simplest cases are difficult or impossible to implement in such calculations. This is not only because of technical reasons, due to the multitude of s.p. levels, and lack of knowledge of the necessary coupling strengths for the sequential transitions involving excited states in the intermediate and final channels, but also there are some more fundamental problems. Namely, excitation of many noncollective levels at the cost of partial dissipation of kinetic energy, being a nonreversible process puts the problem in the field of open quantum systems [21]. While in the conventional CC method, irreversible energy dissipation and couplings to internal degrees of freedom are treated to set in at some point inside the barrier without affecting quantum coherence, in fact this would be a gradually increasing process along the approaching trajectory (see also Ref. [3]). A microscopic description for such process may require something beyond an imaginary potential [22].

In Refs. [23–25], the random matrix model was applied in order to take into account noncollective excitations during fusion reactions. This approach consists of merging a statistical approach with quantum mechanics by extending the CC method using a general random matrix theory (RMT), initially developed by Weidenmüller and collaborators [26]. The RMT is then used for obtaining the coupling form factor between the ground state and noncollective levels in a target nucleus. The method was successfully applied to the ^{20}Ne + ^{90,92}Zr cases [25], where the authors demonstrated that the couplings to many noncollective levels in the systems visibly smoothed the peak structure in the barrier distribution for the ^{20}Ne + ^{92}Zr system while the barrier distribution for the ^{20}Ne + ^{90}Zr system is altered only slightly.

In this paper, we apply this method systematically to the ^{20}Ne + ^{90,92}Zr, ^{58,60,61}Ni, ^{118}Sn, ^{208}Pb systems and discuss the role of dissipation in heavy-ion reactions around the Coulomb barrier in a much wider mass region than in the previous work. To this end, we make a few improvements in the model, e.g., by using theoretical level densities instead of measured ones, which may be limited by energy resolution of experimental instrumentation.

II. CC + RMT MODEL

We perform coupled-channels calculations with noncollective excitations based on Ref. [25]. The standard CC equations in the isocentrifugal approximation read [3]

$$\left[-\frac{\hbar^2}{2\mu}\frac{d^2}{dr^2} + \frac{J(J+1)\hbar^2}{2\mu r^2} + V_{\rm rel}(r) + \epsilon_n - E\right]u_n^J(r) + \sum_m V_{nm}(r)u_m^J(r) = 0, \quad (3)$$

where ϵ_n is the excitation energy for the n^{th} channel and J is the total angular momentum, while μ and $V_{\text{rel}}(r)$ are the reduced mass and the optical potential for the relative motion, respectively. Here, n includes both collective and noncollective states, together with the entrance channel ($n = 0$). For the couplings to collective excitations the coupling matrix elements are calculated according to the collective model to all orders of the coupling constant [3,27]. On the other hand, for the couplings to the noncollective excitations [that is, the coupling matrix elements V_{nm} in Eq. (3)], we employ the random matrix theory. According to it, one considers an ensemble of coupling matrix elements and require that their first moment vanishes, while the second moment is given by the formula developed by Weidenmüller *et al.* (Eq. (2.8) in Ref. [28]). That is, for the coupling between a noncollective state with spin I and a noncollective state with spin I′, one has

$$\overline{V^{II'}_{nn'}(r)} = 0 \tag{4}$$

and

$$\begin{aligned}\overline{V^{II'}_{nn'}(r)V^{I''I'''}_{n''n'''}(r')} = {} & \{\delta_{nn''}\delta_{n'n'''}\delta_{II''}\delta_{I'I'''}+\delta_{nn'''}\delta_{n'n''}\delta_{II'''}\delta_{I'I''}\} \\ & \times\sqrt{(2I+1)(2I'+1)}\sum_{\lambda}\begin{pmatrix} I & \lambda & I' \\ 0 & 0 & 0\end{pmatrix}^2 \\ & \times\alpha_\lambda(n,n';I,I';r,r')\end{aligned} \tag{5}$$

with (for $n' = 0$ and $I' = 0$)

$$\alpha_\lambda(n,0;I,0;r,r') = \frac{w_\lambda}{\sqrt{\rho(\epsilon_n)}}e^{-\frac{\epsilon_n^2}{2\Delta^2}}e^{-\frac{(r-r')^2}{2\sigma^2}}h(r)h(r'). \tag{6}$$

Here, the bars denote an ensemble average, ρ is the level density, and w_λ, Δ, and σ are adjustable parameters. In Ref. [25], the function $h(r)$ is assumed to be the derivative of Woods-Saxon potential. In solving the coupled-channels equations, the coupling matrix elements are randomly generated according to Eqs. (4) and (5) for each value of ε and spin of noncollective level.

In Ref. [25], the Weidenmüller model was applied to excitations within the same nucleus, limited to the target nucleus only (an approximation well justified for systems with projectiles much lighter than the target nuclei). Moreover, in our implementation only couplings from the ground state to noncollective states were taken into account.

In this paper, we will improve the previous calculations of Ref. [25] by taking into account the following points.

(i) The key factor in the RMT approach is the level density $\rho(E)$, where E is the excitation energy. In Ref. [25] the experimental noncollective level densities have been used, while in the present paper it will be replaced by theoretical ones. The reason is that the experimental $\rho(E)$ data are limited by energy resolution of instrumentation. With increasing energy this unavoidably results in losing an ever larger part of level density. Because of this, the level density for ^{92}Zr employed in Ref. [25] has a nonphysical dropping (see Fig. 2 of Ref. [25]), instead of an exponential-like increasing function.

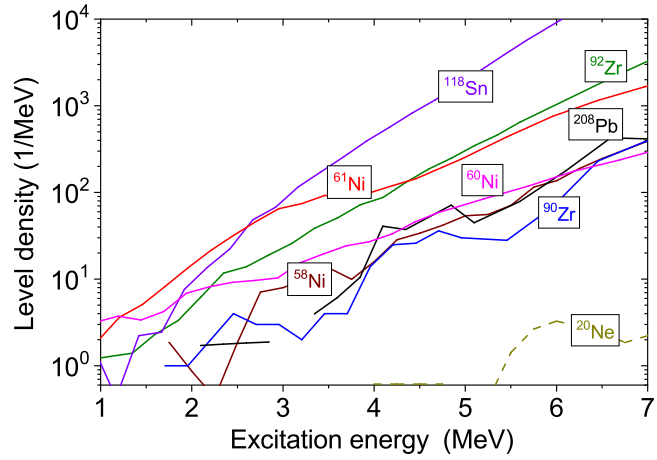

FIG. 1. Theoretical single particle (s.p.) level densities of the relevant nuclei calculated with the Skyrme-Hartree-Fock-Bogoliubov (HFB) method, taken from Refs. [29,30].

For the theoretical level densities, we employ the results of Skyrme-Hartree-Fock-Bogoliubov (HFB) calculations by Goriely *et al.* [29,30], which are shown in Fig. 1. Described there, the combinatorial method consists in using single-particle (s.p.) HFB method to construct incoherent particle-hole state densities, then collective effects are included. Thus multiparticle states are not taken into account.

As one can see in Fig. 1, the level density for the ^{20}Ne nucleus is much smaller than that for the other nuclei, so its noncollective excitations can be safely disregarded.

Besides $\rho(E)$, the model also requires knowledge of energies and spins of s.p. levels. Since at low energies experimental resolution is sufficient for not missing any energy levels, for excitations up to 2.0 MeV we take the experimental energy levels, but above we generate pseudolevels by drawing them out from the theoretical distributions $\rho(E)$. Concerning the spins of s.p. levels, according to the HFB calculations for excitations relevant to our problem their distributions are almost independent of E. On the other hand, we have checked (by shuffling the s.p. levels spin values measured for ^{92}Zr) that the calculated fusion cross sections and barrier distributions are practically independent of them, so we use the s.p. spins taken from Ref. [31], as has been done in Ref. [25].

(ii) With the level density functions so determined, it has turned out that including 35–75 noncollective levels, as was done in Ref. [25], is not sufficient. Depending on the system, we get convergence at 150–200 s.p. levels (up to ∼1000 channels). For ^{90}Zr this corresponds to the maximum excitation energy of 6.5 MeV, while for ^{92}Zr it is 4.2 MeV.

(iii) To compare calculations with the experiment, in distinction with Ref. [25], we do not use the data from a single angle, but those measured at three angles (130°,

TABLE I. The parameters used in the CC+RMT calculations. For the projectile nucleus, ^{20}Ne, we take into account only the rotational excitations of the ground state band. The high energy 3^- vibrational level in this nucleus was omitted since it causes only the adiabatic potential renormalization [3].

	^{20}Ne	^{58}Ni	^{60}Ni	^{61}Ni	^{90}Zr	^{92}Zr	^{118}Sn	^{208}Pb
$E(2^+)$ [MeV]	(rot) 1.633	(vib) 1.454	(vib) 1.333	(vib) 0.964	(vib) 2.186	(vib) 0.93	(vib) 1.229	(vib) 4.07
β_2 (β_4)	0.46 (0.27)	0.1828	0.207	0.24	0.089	0.1027	0.114	0.055
The number of phonons/ rotational states	3	2	2	2	2	2	2	1
$E(3^-)$ vib. [MeV]	5.62	4.475	4.04	3.9	2.75	2.34	2.325	2.615
β_3	0.39	0.19	0.21	0.20	0.211	0.17	0.114	0.11
The number of phonons	0	2	2	2	2	2	2	2
V [MeV]		57.2	57.2	57.2	55.0	62.3	64.1	64.7
r_{ov} [fm]		1.15	1.15	1.15	1.15	1.15	1.18	1.18
a_v [fm]		0.64	0.64	0.64	0.65	0.65	0.66	0.66

140°, and 150°in the laboratory system) after scaling them according to the prescription [6–8].

$$E_{\text{eff}} = \frac{2E_{\text{c.m.}}\sin(\theta_{\text{c.m.}}/2)}{1+\sin(\theta_{\text{c.m.}}/2)}. \tag{7}$$

(iv) Because cyclotron beams having a non-negligible energy resolution were used in the experiments, to compare theory with the experiment we fold theoretical distributions with a Gaussian function of appropriate widths, which influences the results significantly.

(v) Finally, in addition to calculations performed for the ^{20}Ne + ^{90,92}Zr systems, we carry them out also for the ^{58,60,61}Ni, ^{118}Sn, and ^{208}Pb targets. Results of these calculations are compared with our measurements published in Refs. [12,15,17,32,33].

III. CALCULATION PARAMETERS

Concerning the parameters used in the calculations, we avoided any fitting as much as possible and employed the values taken from external sources. Due to this, we will be able to check the predictive power of the model. For the real part of the potentials we assumed the Woods-Saxon shape with parameters V, r_{0v}, and a_v given by the Akyuz-Winther potential [34]. Concerning the imaginary part of the potential, also of the W-S form, we always assumed that it is well localized inside the barrier, using it only to ascertain internal absorption after tunneling the barrier. In our application, with this assumption, the precise values of W, r_{0w}, and a_w (for which we have assumed 30 MeV, 0.9 fm, and 0.5 fm, respectively) have a very weak influence on results. The radius parameter for the couplings is set in all cases to be 1.20 fm. Concerning the deformation parameter of ^{92}Zr according to the Ref. [35] the values of β_2^N of ^{92}Zr = 0.144 or 0.20 give similar fits to the experimental fusion barrier distribution of the ^{16}O + ^{92}Zr system, while according to Ref. [36] the $\beta_2^C = 0.1027$. To our opinion this large difference between β_2^N and β_2^C can be caused by fitting parameters of the CC model not taking into account couplings to the noncollective levels, which could be mocked up by enlarging the β_2^N. Because of this we prefer to assume that $\beta_2^N = \beta_2^C = 0.1027$. The values for the other parameter, taken from Refs. [36–38], are shown in Table I.

A somewhat more complicated was the case of ^{61}Ni. Because this is an odd-A nucleus, the ground-state spin is not 0 and there is no single level with 2^+ in an excited state, as in the ^{58,60}Ni isotopes. Instead, there is a multiplet, formed by the coupling of the valence neutron in the $2p_{3/2}$ orbit with the one-phonon state in ^{60}Ni [39]. As we argued in Ref. [12], in calculations the multiplet is replaced by a single effective state given as a spin average of the multiplet states. In Ref. [12], the energy was calculated well (0.9643 MeV), however, its β_2 value was largely underestimated. The reason is that in such a case the relation between an experimental $B(E2)$ and β_2 is different from that for a transition from the g.s. 0^+ to the 2^+ state in even-even nuclei. A general formula is given in the Appendix and based on it we determined the β_2 for the effective collective state in ^{61}Ni as 0.24(1).

The values for the global RMT parameters in Eq. (6), Δ and σ, were roughly estimated already in the paper of Weidenmüller *et al.*, as 7 MeV and 4 fm, respectively [28], and we took them without any changes as was done in Ref. [25]. In fact, we have checked that results are surprisingly insensitive to values of these parameters. The global coupling strength parameter w_λ was fitted in Ref. [25] as 200 MeV$^{2/3}$. We employed the same value for the systems in our study as well. Since the calculations were computationally very demanding, we have used parallely 50 CPUs of the PL-Grid Infrastructure.

IV. RESULTS

Let us now numerically solve the coupled-channels equations with noncollective excitations and discuss the role of nuclear dissipation. The influence of dissipation on the excitation function of quasielastic backscattering for the ^{20}Ne + ^{90,92}Zr systems is shown in Fig. 2. In this figure, we present a comparison of the results of the CC + RMT calculations with the experimental data published in Ref. [14]. It is seen that, in agreement with expectations, the higher level density of ^{92}Zr influences stronger the shape of the excitation function than in the case of the ^{90}Zr target.

We would like to point out that the internucleus potential, which we use, is a phenomenological one, and there is a

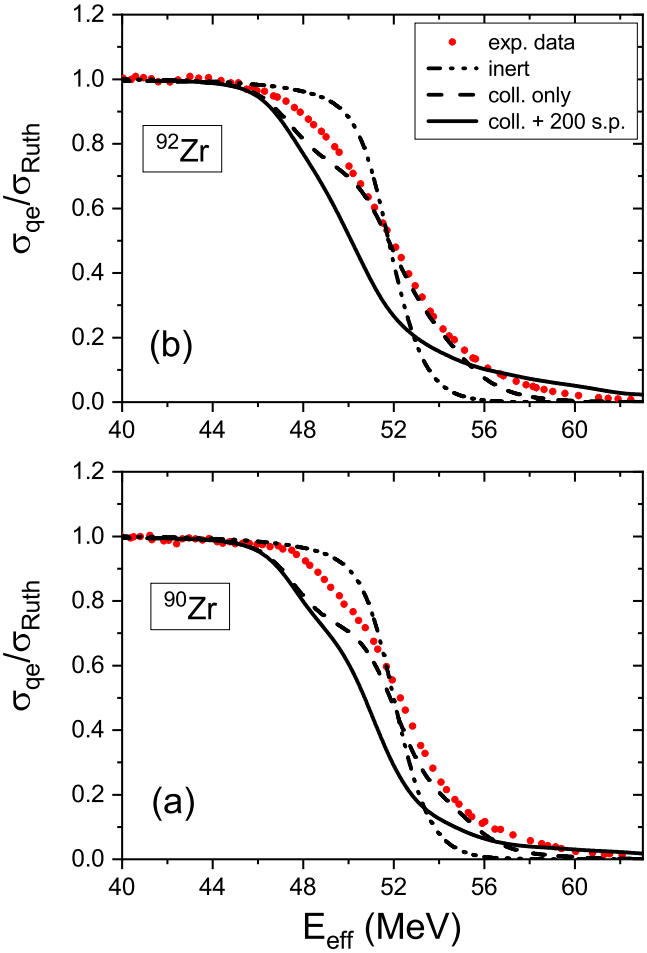

FIG. 2. Excitation functions of quasielastic scattering for the ^{20}Ne + ^{90,92}Zr systems calculated for $\Theta_{\rm c.m.} = 148^\circ$ ($\Theta_{\rm lab} = 140^\circ$). The experimental results (the dots), taken from Ref. [14], were measured at $\Theta_{\rm lab} = 130^\circ$, 140°, and 150°. The dot-dot-dashed curves were calculated without taking into account any couplings, and the dashed curves were calculated by taking into account only the collective excitations of the projectile and target nuclei. The solid lines show the results with the additional including of 200 s.p. excitations.

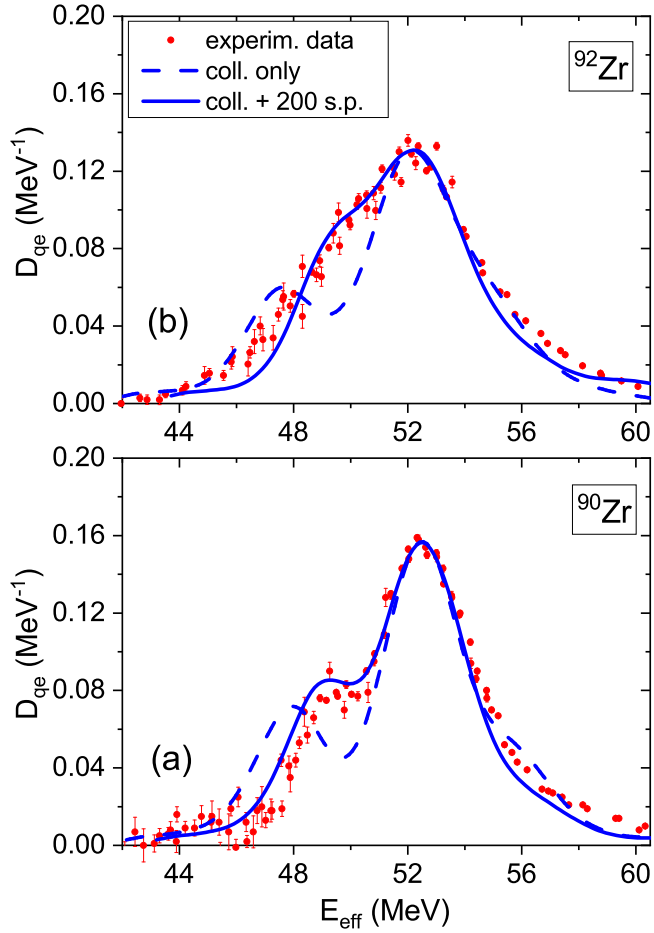

FIG. 3. Experimental (points) and theoretical quasielastic barrier distributions (BDs) for the ^{20}Ne + ^{90,92}Zr systems. The dashed curves show results of the standard CC calculations taking into account the collective excitations only. The solid curves show the results of including in addition 200 s.p. excitations in the target nuclei. The experimental energy resolution of 1.2 MeV was taken into account by folding the calculated distributions with a Gaussian function of this FWHM. Since we are more interested in the shapes than the absolute positions of BD, the theoretical curves were normalized to the experimental data in the peaks, and also shifted to higher energy by 1.3 MeV – 1.6 MeV. The experimental data are taken from Ref. [14].

freedom to change the parameters of the potential depending on the model space employed in a calculation. That is, if we include the noncollective excitations, in principle, we would have to change the potential parameters in order to reproduce the experimental data, e.g., changing the r_{0v} parameter from 1.15–1.2 fm. However, we do not want to fit any parameters to have some predictive possibilities. In general, the coupling to states with large excitation energy leads to a shift of fusion excitation function. This is referred to as a barrier renormalization [3,40]. One important thing is that such a change in the potential parameters mainly changes the height of the Coulomb barrier (if we keep the diffuseness parameter to be the same), which can be well mocked up by shifting the excitation function. It is important that the change in the real potential parameters does not influence much the shape of barrier distribution, that is what interests us in this paper, even though the absolute values of cross sections are altered.

To better see the evolution of barrier distributions after adding two neutrons to ^{90}Zr and after switching on dissipation, Fig. 3 plots the corresponding quasielastic barrier distributions. The effect of noncollective excitations is qualitatively the same as in the previous calculations presented in Ref. [25].

In Fig. 4 we show the corresponding comparison of BD for the ^{20}Ne + ^{58,60,61}Ni systems. The influence of noncollective excitations (dissipation) on barrier distributions is clearly seen: the barrier distributions are evidently smoothed in comparison with CC expectations, moreover, without any fitting the calculated BD agree with experimental results.

In contrast, there is no agreement for the ^{20}Ne + ^{118}Sn and ^{20}Ne + ^{208}Pb systems, as shown in Figs. 5 and 6. The possible reason can be that the width of the barrier distribution

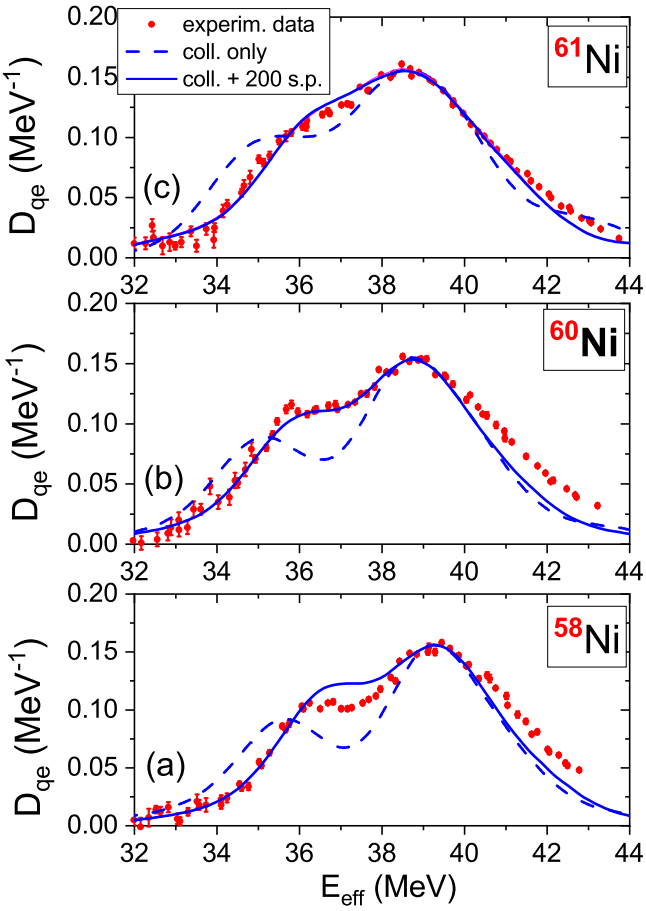

FIG. 4. Experimental (points) and theoretical barrier distributions for the ^{20}Ne + ^{58,60,61}Ni. The dashed lines show results of the standard CC calculations taking into account couplings to the collective excitations only, and the solid lines were obtained after including also couplings to 200 noncollective ones. This corresponds to excitation energy up to 6.2 MeV in ^{58,60}Ni and 4.2 MeV in ^{61}Ni. The experimental resolution of 1.0 MeV (FWHM) was taken into account. The β_2 value of 0.24 for the ^{61}Ni target (see text) was critically important to achieving agreement between the experimental data and the calculations. To overlap the experimental and calculated peaks we shifted the latter ones to higher energy by 0.1–1.0 MeV. The experimental data originate from Ref. [12].

is approximately proportional to the product of the projectile and target atomic numbers [1], which can be called Coulomb zoom. Due to this for heavier targets the standard CC calculations predict the structure peaks so far away, that in spite of the high level density of the ^{118}Sn nucleus (see Fig. 1) couplings to s.p. excitations are not sufficient to smooth out the structure completely, even though the peak-to-valley ratio in the calculated distribution is significantly decreased due to dissipation. Notice that similar (no structure) experimental distributions were observed for other Sn isotopes as well [32,33].

Also in the case of ^{20}Ne + ^{208}Pb we observed the smooth Gaussian-like barrier distribution (of both experimental $D_{\rm qe}$ and $D_{\rm fus}$) [15], although for this system, the doubly magic target nucleus ^{208}Pb has so low level density that according

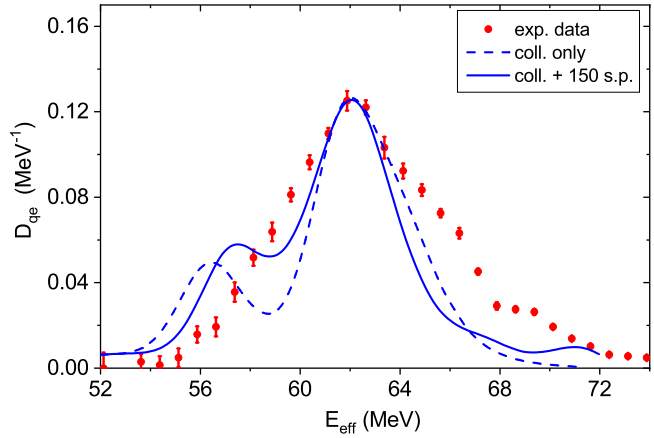

FIG. 5. Experimental (points) and theoretical barrier distributions for the ^{20}Ne + ^{118}Sn system. The dashed line show results of the standard CC calculations taking into account the couplings to the collective levels only, and the solid line was obtained after including also couplings to 150 s.p. ones, what corresponds to excitation energies up to 3.7 MeV. The experimental resolution of 1.5 MeV (FWHM) was taken into account. The calculated distributions were normalized and shifted (by ∼0.5 MeV) to overlap the peaks. The experimental data (for $\Theta_{\rm c.m.} = 135^\circ$, 145°, and 155°) are taken from Refs. [32,33].

to the calculations one would expect a prominent structure in the barrier distribution (Fig. 6). In this situation the only weak reaction channels that could be responsible for the BD widening and complete smoothing of the structure could be the transfer ones. In fact, according to our measurements [15] the transfer cross sections in ^{20}Ne + ^{118}Sn and particularly in ^{20}Ne + ^{208}Pb are much stronger than that for the lighter targets.

The predicted effect of dissipation on fusion cross sections for the ^{20}Ne + ^{90,92}Zr systems is shown in Figs. 7–10 for

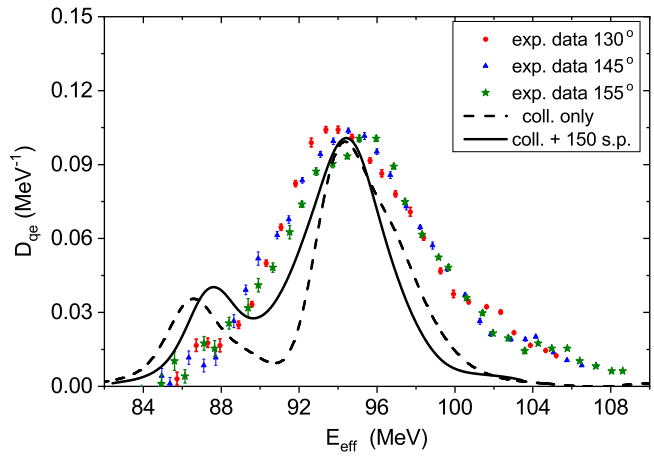

FIG. 6. The same as Fig. 5, but for the ^{20}Ne + ^{208}Pb system. 150 s.p. levels corresponds to excitation energies up to 6.1 MeV. The experimental resolution of 0.7 MeV (FWHM) was taken into account. The experimental data taken from Ref. [15].The calculated distributions were normalized and shifted (by ∼1.3 MeV) to overlap the peaks.

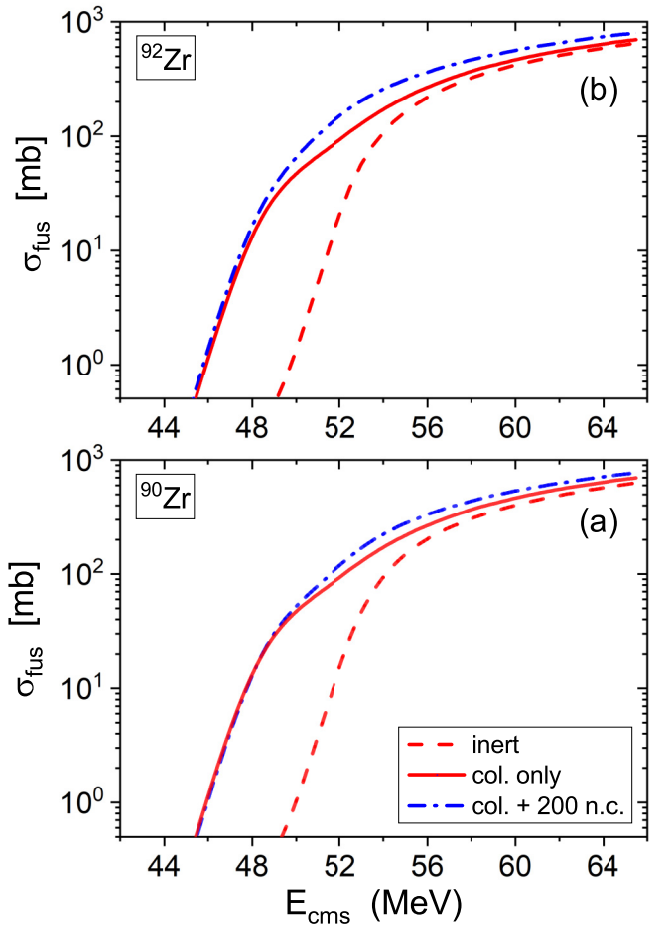

FIG. 7. Fusion excitation functions for the ^{20}Ne + ^{90,92}Zr systems calculated with several coupling schemes. The red dashed lines were obtained without any couplings. The red solid lines were obtained by taking into account couplings to the collective levels, while the blue dash-dot lines show the results with including dissipation: 200 s.p. levels.

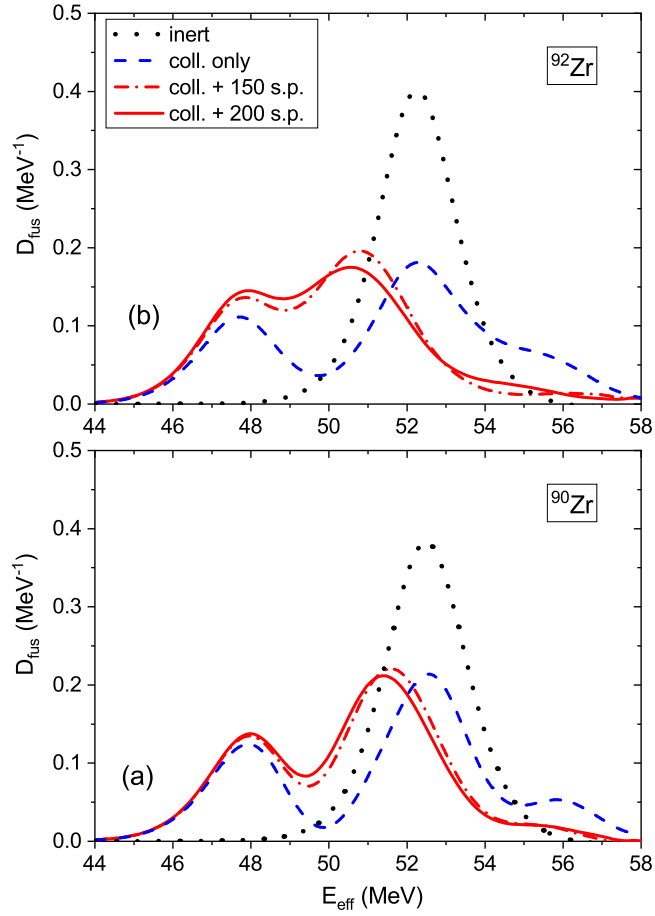

FIG. 8. Fusion barrier distributions $D_{\rm fus}$ of the ^{20}Ne + ^{90,92}Zr systems. The black dotted lines show the distributions calculated without any couplings taken into account, the blue dashed lines were calculated with collective excitation included. The red dash-dot and solid lines show results of including 150 and 200 s.p. levels, correspondingly.

which the calculations were performed with the parameters given in Table I. Since they are not compared to experimental data, neither energy shifts nor resolution corrections were applied.

It is seen that couplings to s.p. levels modify quasielastic and fusion barrier distributions to different extent, which is caused by different resolution of theoretical test functions (1) and (2), however, their maxima are at the same energy. The effect of coupling to collective and noncollective levels on the fusion barrier penetrability is shown in Fig. 10.

The penetrability is proportional to the derivative of the product of E and fusion cross section:

$$P \sim \frac{d(E\sigma_{\rm fus}(E))}{dE}$$

and is seen (Fig. 10) that, according to the CC + RMT model, it is enhanced below the barrier (∼52 MeV) due to the couplings to s.p. levels.

V. DISCUSSION

Even though the standard coupled-channels method appears to be successful for many heavy-ion fusion reactions [3], one has to be aware that several assumptions and approximations are used in this approach. Some of them are listed below:

(i) Ambiguities and uncertainties of the optical model parameters: a particularly difficult problem concerning the imaginary part of the internuclear potential, which is rather a measure of our ignorance and model approximations;
(ii) Disregarding energy and angular momentum dependences in an internuclear potential;
(iii) Uncertainty of coupling length parameters $\delta = R_{\rm coupl}\beta$, where $R_{\rm coupl}$ is not necessarily the same as the charge or the matter radii. Also, the nuclear deformation parameter β_2^N is not necessarily the same as the electromagnetic deformation parameter β_2^C, which can be estimated (usually to the first order only, though) from the electromagnetic transition strengths,

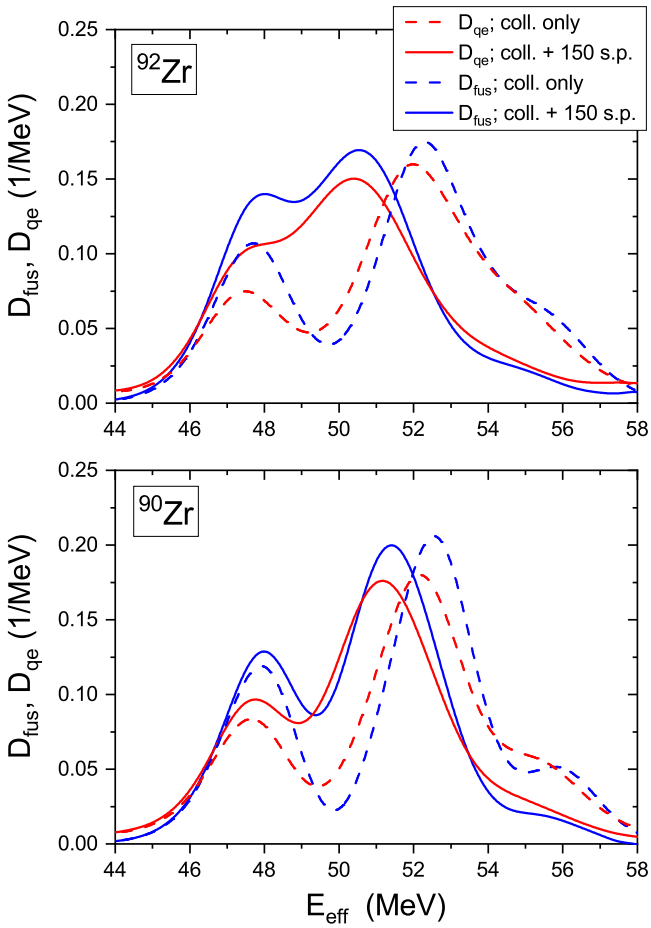

FIG. 9. Comparison of $D_{\rm fus}$ and $D_{\rm qe}$ (calculated for 152 deg. in c.m. frame) for the ^{20}Ne + ^{90,92}Zr systems calculated with couplings to collective (dashed lines) and collective + 150 single-particle excitation levels (solid lines) in target nuclei taken into account. No energy shifts neither experimental resolution corrections were applied.

$B(E\lambda)$. Even the sign of deformation is not always known for deformed nuclei, and collective excitations

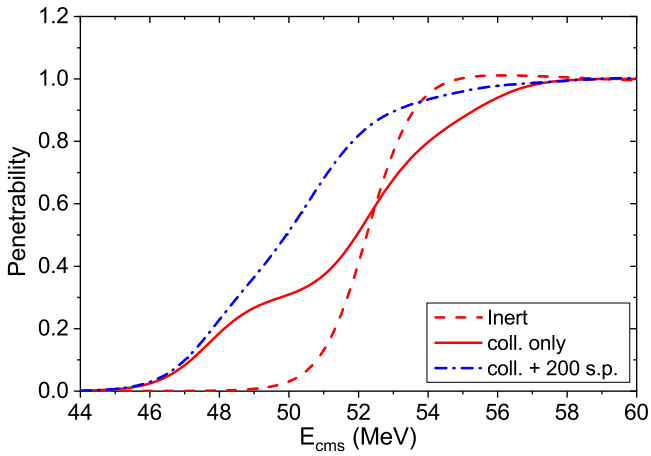

FIG. 10. Barrier penetrability for the ^{20}Ne + ^{92}Zr as a function of the projectile energy in the center-of-mass frame for the same conditions as in Fig. 7.

are not always clearly rotational or vibrational (see also Refs. [41,42]);

(iv) Disregarding the axially asymmetric deformations and deformation softness [43];

(v) Disregarding some degrees of freedom (such as transfer channels and noncollective excitations), difficult to take into account.

This incomplete list may be increased by some approximations of the particular codes, as, e.g., disregarding some types of couplings or the isocentrifugal approximation, which strongly speeds up the CC calculations and works well for sub-barrier fusion and backward scattering, but is good for some angular range only [7].

The list would provide some idea on the significance of fits to limited sets of data, e.g., of the CC calculations for barrier distributions for some particular projectile+target system. It is true that not all factors influence observables in a similar way. For instance, looking for a reason of smoothing out the structure of $D_{\rm qe}$ in ^{20}Ne + ^{208}Pb we have found (see Fig. 4 in Ref. [14]) that of all optical model parameters only changing r_{ow} leads to agreement between the experiment and theory. However, it would be difficult to extract the physics behind such a fit. Moreover, such an approach hardly gives us the predictive power, giving us at best only a way of parametrizing the data.

Because of this, in our studies, we have taken another strategy choosing some special combinations of the projectile and the target nuclei fulfilling the following criteria:

(i) The shape of barrier distribution (calculated in the framework of the standard CC model) should be structured and dominated by the projectile nucleus, i.e., by its large deformation, so changing targets should not change significantly the shape of the barrier distribution calculated without taking into account dissipation.

(ii) The dissipation should concern mainly the target nucleus (i.e., it should have much higher level density than the projectile, which means that the target should be significantly heavier than the projectile).

(iii) The transfer probability (mainly $1n$ and $2n$ transfer channels) should be as low as possible, otherwise it would highly complicate interpretation of results.

One should stress, however, that the CC + RMT model itself also has its own approximations, among others:

(i) The Weidenmüller's coupling form factor (Eq. (2.8) in Ref. [28]) was further approximated in Ref. [25]. In fact for single-particle excitations a more reasonable form of $h(r)$ would be the one that is proportional to the overlap between two single-particle wave functions (for an initial and a final states).

(ii) Noncollective excitations are taken into account only in the target nuclei (this approximation is justified when there is a large difference in s.p. level densities between the projectile and the target nuclei).

(iii) Level densities are theoretical ones. Since we are not aware of any multiparticle theoretical level densities,

we used the tables giving densities of single-particle levels. While they are normalized to experimental values at ∼8 MeV, at critical excitation energy 3–5 MeV their uncertainty is difficult to estimate, which may reach even 50% [44]. We checked, however, that this uncertainty does not significantly influence the shape of barrier distributions.

(iv) The spin values of individual s.p. pseudolevels could be drawn from the HFB tables [29,30], however, we checked that the spin distributions, according to the HFB calculations, are not strongly dependent on excitation energy in the range considered in this paper. Moreover, according to our tests, shuffling the spin values practically does not influence barrier distributions.

(v) In the CC + RMT model only the couplings between s.p. levels and its ground state in the target are taken into account. In particular couplings among noncollective states are disregarded. Of course such couplings are of second order, but with the exponentially rising level density this approximation may start to be questionable, especially in heavier targets, with high level density even at relatively low excitations.

(vi) The number of noncollective excitations is limited by computer resources. For the systems discussed in this paper, the results have already converged, however, for targets with higher level densities one probably has to increase the number of excited levels to be included in the calculations. Perhaps this will require other numerical methods and/or much more powerful computing infrastructure.

Last, but certainly not least: it is assumed that the problem can be described by the stationary Schrödinger equation, while the time-dependent approach may be more convenient for irreversible processes [21].

VI. CONCLUSIONS

Influence of dissipation on tunneling becomes a well-established phenomenon, with ever stronger support both from the experimental as well as the theoretical sides. In our view, determination of physical parameters using the CC codes without taking into account weakly coupled channels may be in many cases, especially for heavy targets, disputable.

From the list shown in the previous section, it is seen that there are a lot of places for improvement in the CC + RMT model for treatment of dissipation effects on tunneling. Taking into account assumptions and approximations used, as well as uncertainties of parameters, quantitative agreement presented in this paper between the CC+ RMT calculations and the experimental results for the ^{20}Ne + ^{90,92}Zr and ^{20}Ne + ^{58,60,61}Ni systems can be considered surprisingly good. Because it was obtained without fitting parameters for individual systems, the predictive power of the model is promising and should be checked with other systems. Measurements of barrier distributions for ^{24}Mg + ^{90,92}Zr as well as transfer measurements for these systems have already been performed and preliminary results have been published [45,46]. Our preliminary calculations indicate that also in this case the influence of couplings to noncollective levels is sufficient to explain differences between the barrier distribution for the ^{24}Mg + ^{90,92}Zr systems. On the other hand, the CC + RMT model apparently is not sufficient to explain the Gaussian-like shapes of barrier distributions for the ^{20}Ne + ^{118}Sn and ^{20}Ne + ^{208}Pb, so in these systems the transfer reactions probably dominate modification of barrier distributions.

ACKNOWLEDGMENTS

This work was supported by the National Science Centre under Contracts No. UMO-2013/08/M/ST2/00257 and No. UMO-2014/14/M/ST2/00738. This research was also supported in part by the PL-Grid Infrastructure.

APPENDIX: DEFORMATION PARAMETER FOR ODD-MASS NUCLEI IN THE WEAK COUPLING MODEL

In this Appendix, we derive the relation between a deformation parameter and probability of electromagnetic transitions for odd-mass nuclei, for which the ground-state spin is a half-integer. To this end, we assume that the structure of an odd-mass nucleus is well described with a weak coupling model, in which the valence nucleon is weakly coupled to the even-even core nucleus. That is, the wave function of a state with spin I and its z component M reads,

$$|IM\rangle = \left[\left|\phi_{I_c}\right\rangle \otimes |\psi_{jl}\rangle\right]^{(IM)}, \tag{A1}$$

where ϕ_{I_c} is the wave function for the core nucleus with the spin I_c while ψ_{jl} is the single-particle wave function for the valence nucleon with the total and the orbital angular momenta of j and l, respectively.

The electric transition probability from the state I to the state I' is in general defined as

$$B(E\lambda; I \to I') = \frac{1}{2I+1} |\langle I||\hat{T}_{E\lambda}||I'\rangle|^2, \tag{A2}$$

where $\hat{T}_{E\lambda}$ is the operator for the $E\lambda$ transition. Assuming that the operator $\hat{T}_{E\lambda}$ acts only on the core nucleus, we obtain

$$\langle I||\hat{T}_{E\lambda}||I'\rangle = \left\langle \left[\phi_{I_c} \otimes \psi_{jl}\right]^{(I)} \middle|\middle| \hat{T}_{E\lambda} \middle|\middle| \left[\phi_{I'_c} \otimes \psi_{jl}\right]^{(I')} \right\rangle, \tag{A3}$$

$$= (-)^{I_C+j+I'+\lambda}\sqrt{(2I+1)(2I'+1)} \times \begin{Bmatrix} I_c & I & j \\ I' & I'_c & \lambda \end{Bmatrix} \left\langle \phi_{I_c} \middle|\middle| \hat{T}_{E\lambda} \middle|\middle| \phi_{I'_c} \right\rangle, \tag{A4}$$

where we have used Eq. (7.1.7) in Ref. [47].

For the transition from the one phonon states to the ground state in an odd-mass nucleus, one has $I_c = \lambda$, $I'_c = 0$, and $I' = j$. Using

$$\begin{Bmatrix} \lambda & I & j \\ j & 0 & \lambda \end{Bmatrix} = (-)^{I+\lambda+j} \frac{1}{\sqrt{(2\lambda+1)(2j+1)}}, \tag{A5}$$

and the relation between the $B(E\lambda)$ value and the deformation parameter β_λ [3,27], that is,

$$|\langle I_C = \lambda||\hat{T}_{E\lambda}||I'_C = 0\rangle|^2 = \left(\frac{3e}{4\pi} Z R^\lambda\right)^2 \beta_\lambda^2, \tag{A6}$$

where Z and R are the proton number and the radius of the core nucleus, respectively, one then obtains

$$B(E\lambda; I \rightarrow \text{g.s.}) = \frac{1}{2\lambda+1}\left(\frac{3e}{4\pi}ZR^{\lambda}\right)^2 \beta_{\lambda}^2. \quad \text{(A7)}$$

From this relation, one finally obtains

$$\beta_{\lambda} = \frac{4\pi}{3ZR^{\lambda}}\sqrt{\frac{(2\lambda+1)B(E\lambda; I \rightarrow \text{g.s.})}{e^2}}. \quad \text{(A8)}$$

For the ^{61}Ni nucleus, the ground state has spin parity of $I^{\pi} = 3/2^{-}$. This is interpreted as the valence neutron in the $p_{3/2}$ state coupled to the ground state of ^{60}Ni [39,48]. The one quadrupole phonon states in ^{61}Ni are the first 2^{+} state in ^{60}Ni coupled to the valence neutron in the $p_{3/2}$ state. This leads to the total spin of $I = 1/2^{-}, 3/2^{-}, 5/2^{-}$, and $7/2^{-}$. We assume that these are the $I = 1/2^{-}$ state at 656 keV, the $3/2^{-}$ state at 1100 keV, the $5/2^{-}$ state at 909 keV, and the $7/2^{-}$ state at 1014 keV. The measured electric transition probabilities from the ground state to those states [48] as well as the estimated deformation parameters are summarized in Table II. The effective deformation parameter for the one phonon states [12] is then obtained as $\beta_{\text{eff}} = \sqrt{\sum_i \beta_{2i}^2} = 0.236$.

TABLE II. The measured excitation energies and the $E2$ transition probabilities [48] for the one phonon states in ^{61}Ni. The last column shows the deformation parameters β_2 estimated with Eq. (A8), using the radius of $R = 1.2 \times 60^{1/3}$ fm. Notice that the $B(E2)\downarrow$ is related to the $B(E2)\uparrow$ as $B(E2)\downarrow = (2I_{\text{g.s.}}+1)B(E2)\uparrow/(2I+1)$.

I^{π}	Excitation energy (keV)	$B(E2)\uparrow$ (e^2fm^4)	β_2
$1/2^{-}$	656	64(5)	0.169
$5/2^{-}$	909	65(5)	0.0986
$5/7^{-}$	1014	78(6)	0.0936
$3/7^{-}$	1100	39(3)	0.0936

[1] M. Dasgupta, D. J. Hinde, N. Rowley, and A. M. Stefanini, Annu. Rev. Nucl. Part. Sci. **48**, 401 (1998).
[2] B. B. Back, H. Esbensen, C. L. Jiang, and K. E. Rehm, Rev. Mod. Phys. **86**, 317 (2014).
[3] K. Hagino and N. Takigawa, Prog. Th. Phys. **128**, 1061 (2012).
[4] A. M. Stefanini, D. Ackermann, L. Corradi, D. R. Napoli, C. Petrache, P. Spolaore, P. Bednarczyk, H. Q. Zhang, S. Beghini, G. Montagnoli, L. Mueller, F. Scarlassara, G. F. Segato, F. Soramel, and N. Rowley, Phys. Rev. Lett **74**, 864 (1995).
[5] N. Rowley, G. R. Satchler, and P. H. Stelson, Phys. Lett. B **254**, 25 (1991).
[6] H. Timmers,, J. R. Leigh, M. Dasgupta, D. J. Hinde, R. C. Lemmon, J. C. Mein, C. R. Morton, J. O. Netwon, and N. Rowley, Nucl. Phys. A **584**, 190 (1995).
[7] K. Hagino and N. Rowley, Phys. Rev. C **69**, 054610 (2004).
[8] L. F. Canto, P. R. S. Gomes, R. Donangeloa, and M. S. Hussein, Phys. Rep. **424**, 1 (2006).
[9] J. O. Newton, R. D. Butt, M. Dasgupta, D. J. Hinde, I. I. Gontchar, C. R. Morton, and K. Hagino, Phys. Rev. C **70**, 024605 (2004).
[10] J. O. Newton, R. D. Butt, M. Dasgupta, D. J. Hinde, I. I. Gontchar, C. R. Morton, and K. Hagino, Phys. Lett. B **586**, 219 (2004).
[11] A. Mukherjee, D. J. Hinde, M. Dasgupta, K. Hagino, J. O. Newton, and R. D. Butt, Phys. Rev. C **75**, 044608 (2007).
[12] A. Trzcińska, E. Piasecki, K. Hagino, W. Czarnacki, P. Decowski, N. Keeley, M. Kisieliński, P. Koczoń, A. Kordyasz, E. Koshchiy, M. Kowalczyk, B. Lommel, A. Stolarz, I. Strojek, and K. Zerva, Phys. Rev. C **92**, 034619 (2015).
[13] A. Trzcińska, E. Piasecki, A. Amar, W. Czarnacki, N. Keeley, M. Kisieliński, S. Kliczewski, M. Kowalczyk, B. Lommel, M. Mutterer, R. Siudak, A. Stolarz, I. Strojek, G. Tiourin, and W. H. Trzaska, Phys. Rev. C **93**, 054604 (2016).
[14] E. Piasecki, Ł. Świderski, W. Gawlikowicz, J. Jastrzębski, N. Keeley, M. Kisieliński, S. Kliczewski, A. Kordyasz, M. Kowalczyk, S. Khlebnikov, E. Koshchiy, E. Kozulin, T. Krogulski, T. Loktev, M. Mutterer, K. Piasecki, A. Piórkowska, K. Rusek, A. Staudt, M. Sillanpää, S. Smirnov, I. Strojek, G. Tiourin, W. H. Trzaska, A. Trzcińska, K. Hagino, and N. Rowley, Phys. Rev. C **80**, 054613 (2009).
[15] E. Piasecki, Ł. Świderski, N. Keeley, M. Kisieliński, M. Kowalczyk, S. Khlebnikov, T. Krogulski, K. Piasecki, G. Tiourin, M. Sillanpää, W. H. Trzaska, and A. Trzcińska, Phys. Rev. C **85**, 054608 (2012).
[16] E. Piasecki, W. Czarnacki, N. Keeley, M. Kisieliński, S. Kliczewski, A. Kordyasz, M. Kowalczyk, S. Khlebnikov, E. Koshchiy, T. Krogulski, T. Loktev, M. Mutterer, A. Piórkowska, K. Rusek, M. Sillanpää, A. Staudt, I. Strojek, S. Smirnov, W. H. Trzaska, and A. Trzcińska, Phys. Rev. C **85**, 054604 (2012).
[17] E. Piasecki, M. Kowalczyk, K. Piasecki, Ł. Świderski, J. Srebrny, M. Witecki, F. Carstoiu, W. Czarnacki, K. Rusek, J. Iwanicki, J. Jastrzębski, M. Kisieliński, A. Kordyasz, A. Stolarz, J. Tys, T. Krogulski, and N. Rowley, Phys. Rev. C **65**, 054611 (2002).
[18] A. V. Karpov, V. A. Rachkov, and V. V. Samarin, Phys. Rev. C **92**, 064603 (2015).
[19] V. V. Sargsyan, G. G. Adamian, N. V. Antonenko, W. Scheid, and H. Q. Zhang, Phys. Rev. C **91**, 014613 (2015).
[20] V. V. Sargsyan, G. G. Adamian, N. V. Antonenko, W. Scheid, and H. Q. Zhang, Phys. Rev. C **95**, 054619 (2017).
[21] A. Diaz-Torres, Phys. Rev. C **82**, 054617 (2010).
[22] A. Diaz-Torres, Phys. Rev. C **81**, 041603(R) (2010).
[23] S. Yusa, K. Hagino, and N. Rowley, Phys. Rev C **82**, 024606 (2010).
[24] S. Yusa, Ph.D. thesis, Tohoku University, 2013 (unpublished).
[25] S. Yusa, K. Hagino, and N. Rowley, Phys. Rev. C **88**, 054621 (2013).
[26] C. M. Ko, H. J. Pirner, and H. A. Weidenmüller, Phys. Lett. B **62**, 248 (1976).
[27] K. Hagino, N. Rowley, and A. T. Kruppa, Comput. Phys. Commun. **123**, 143 (1999).
[28] D. Agassi, C. M. Ko, and H. A. Weidenmüller, Ann. Phys. (NY) **107**, 140 (1977).

[29] S. Goriely, S. Hilaire, and A. J. Koning, Phys. Rev. C **78**, 064307 (2008).
[30] S. Goriely, http://www-nds.iaea.org/RIPL-3.
[31] http://www.nndc.bnl.gov/ensdf/.
[32] L. Swiderski, P. Czosnyka, M. Kowalczyk, E. Piasecki, K. Piasecki, M. Witecki, J. Jastrzebski, A. Kordyasz, M. Kisielinski, T. Krogulski, N. Rowley, C. Marchetta, A. Pagano, M. Mutterer, W. H. Trzaska, and K. Hagino, Int. J. Mod. Phys. **E13**, 315 (2004).
[33] E. Piasecki, Ł. Świderski, P. Czosnyka, M. Kowalczyk, K. Piasecki, M. Witecki, T. Czosnyka, J. Jastrzębski, A. Kordyasz, M. Kisieliński, T. Krogulski, M. Mutterer, S. Khlebnikov, W. Trzaska, K. Hagino, and N. Rowley, Phys. Lett. B **615**, 55 (2005).
[34] O. Akyüz and A. Winther, Nuclear structure and heavy-ion collisions, in *Proceedings of the International School of Physics, Varenna, Italy, 1979*, edited by R. A. Broglia, C. H. Dasso, and R. Ricci (North-Holland Pub. Co., Amsterdam, 1981).
[35] J. O. Newton, C. R. Morton, M. Dasgupta, J. R. Leigh, J. C. Mein, D. J. Hinde, H. Timmers, and K. Hagino, Phys. Rev. C **64**, 064608 (2001).
[36] S. Raman, At. Data and Nucl. Data Tabl. **78**, 1 (2001).
[37] G. S. Blanpied, B. G. Ritchie, M. L. Barlett, R. W. Fergerson, G. W. Hoffmann, J. A. McGill, and B. H. Wildenthal, Phys. Rev. C **38**, 2180 (1988).
[38] T.Kibedi and R. H.Spear, At. Data Nucl. Data Tables **80**, 35 (2002).
[39] R. Wadsworth, A. Kogan, P. R. G. Lornie, M. R. Nixon, H. G. Price, and P. J. Twin, J. Phys. G **3**, 35 (1977).
[40] K. Hagino, N. Takigawa, M. Dasgupta, D. J. Hinde, and J. R. Leigh, Phys. Rev. Lett. **79**, 2014 (1997).
[41] K. Hagino and G. Scamps, Phys. Rev. C **92**, 064602 (2015).
[42] J. M. Yao and K. Hagino, Phys. Rev. C **94**, 011303(R) (2016).
[43] A. Iwamoto and N. Takigawa, Phys. Lett. B **219**, 176 (1989).
[44] S. Goriely (private communication).
[45] A. Trzcińska, E. Piasecki, M. Kowalczyk, G. Cardella, E. D. Filippo, D. Dell'aquila, S. D. Luca, B. Gnoffo, G. Lanzalone, I. Lombardo, C. Maiolino, N. Martorana, S. Norella, A. Pagano, E. V. Pagano, M. Papa, S. Pirrone, G. Politi, L. Quattrocchi, F. Rizzo, P. Russotto, A. Trifiro, M. Trimarchi, and M. Vigilante, Acta Phys. Pol. B **49**, 393 (2018).
[46] D. Wójcik, A. Trzcińska, E. Piasecki, M. Kisieliński, M. Kowalczyk, M. Wolińska-Cichocka, C. Bordeanu, B. Gnoffo, H. Jia, C. Lin, N. S. Martorana, M. Mutterer, E. V. Pagano, K. Piasecki, P. Russotto, L. Quatrocchi, W. H. Trzaska, G. Tiurin, R. Wolski, and H. Zhang, Acta Phys. Pol. B **49**, 387 (2018).
[47] A. R. Edmonds, *Angular Momenta in Quantum Mechanics* (Princeton University Press, Princeton, 1957).
[48] P. N. Patrawale and R. G. Kulkarni, J. Phys. G **3**, 401 (1977).